ID 1693

LOW VELOCITY IMPACT RESPONSE OF FOAM CORE SANDWICH COMPOSITES - II

M. Motuku[*1], U.K. Vaidya[2], R.M. Rodgers[1], and S. Jeelani[1]

[1] *Center for Advanced Materials (T-CAM), Tuskegee University, Tuskegee, AL 36088, USA*

[2] *Composite Research Laboratory, North Dakota State University, Fargo, ND 58105, USA*

SUMMARY: The effect of foam core density and facesheet thickness on the low velocity impact response and damage evolution in homogeneous foam core sandwich composites was studied. The failure characteristics, initiation and evolution of damage as well as the effect of impact energy were investigated. Three types of foam cores with different densities, namely Airlite B12.5, Rohacell IG-71 and Airex R63.5, were used to study the effect of core density. Considering four groups of facesheets made of different layers of cross-ply carbon prepregs performed the effect of facesheet thickness. Instron 8210-Drop Weight Impact Test Machine was utilized to conduct the low-velocity impact tests. Comparing the impact load histories, impact plots and failure characteristics performed characterization of the impact response. Fractography analysis was conducted through the use of scanning electron microscopy (SEM) and optical microscopy.

The failure characteristics included facesheet damage in the form of indentation of the upper skin and fiber breakage; core failure (localized crushing in the form of a V-notched groove and distributed compression of the core), delamination and core fracture just below the core-facesheet interface. The threshold facesheet thickness ($t_{threshold}$), critical facesheet thickness ($t_{critical}$), threshold impact energy $(E_{imp})_{threshold}$, and critical impact energy ($E_{critical}$) were identified from the impact plots. The impact parameters varied either linearly or parabolically with impact energy depending on the impact energy, type of foam core and facesheet thickness. Excellent repeatability of impact data was generally obtained with increase in foam core density and facesheet thickness.

KEYWORDS: Threshold Facesheet Thickness, Critical Facesheet Thickness, Threshold Impact Energy, Core Fracture, Sandwich Composites and Low Velocity Impact

INTRODUCTION

Sandwich composites have found greater applications in transport, aircraft, automotive, marine, and defense industries both as structural and functional elements. They are appealing to these industries for structural use because of their high flexural stiffness and lightweight qualities.

Most of the work to date in the area of sandwich composites has been primarily on homogeneous structures; those made of one type of core material and facesheet type per structure [1-4]. Earlier sandwich composites used metallic facesheets before emphasis was placed on composite materials. Graphite/epoxy and fiberglass/epoxy are commonly now used as facesheet materials, between which cores of differing architecture such as honeycomb or lightweight foam materials are sandwiched [3]. The choice of a core material can range from natural structures such as balsa wood and bone, natural replicas such as honeycomb structures,

[*] Molefi Motuku, Assistant Professor and corresponding author; phone: +1 (334) 727-8950 and email: africam@hotmail.com.
Uday K. Vaidya, Associate Professor.
Renee M. Rodgers, Ph.D. Student.
Shaik Jeelani, Professor and Director of T-CAM.

to purely synthetic foam cores made of thermoplastic or thermoset polymer systems [5]. The selection of a core material for a specific application is most often based on material properties critical for optimal service performance. Many issues such as reduction in defense spending, concerns regarding cost optimization, internal and external environmental issues, and increased availability have initiated studies on secondary material properties such as temperature resistance, damping ability, solvent resistance for optimized manufacturing, and material composition that enables recycling [5]. Studies on fundamental issues such as the mechanical behavior of sandwich composites have been investigated for more than a decade [1, 2]. The feasibility of stacking layers of different low-density rigid foam core materials and use of soft integral foams to control cushioning and in acoustic attenuation and sonar damping, and to optimize material utilization has been investigated [5].

In this study, the room-temperature low velocity impact (LVI) response and damage evolution in homogeneous foam core sandwich composites was investigated. The LVI was investigated as a function of foam core density, facesheet thickness, and impact energy through analysis of impact load histories, impact plots and failure characteristics. The initiation and evolution of damage, and the corresponding failure characteristics were characterized by using optical microscopy and SEM.

MATERIALS AND TESTING

Materials

Three different types of foam cores (namely Airex R63.5, Airlite B12.5, and Rohacell IG-71), which are representative of high performance application cores such as those encountered in the aerospace and marine industries, were used in this study. The foam cores were chosen because of their superior impact and fatigue resistance, acoustical characteristics, damage tolerance, excellent cost effectiveness, lightweight, and ability to be affordably manufactured [5-8]. Most representative core types specified by manufacturers as damage resistant/high impact resistant cores were considered in this study.

Airex R63.5 is linear PVC foam designed for high quality sandwich of dynamically loaded construction [6]. Airlite B12.5, also referred to as Baltek foam, is cross-linked type foam made from Herex® C70 buns for stiffness, it is more resilient, and offers a high-quality sandwich construction [7]. It is less brittle than other PVC's, and not affected by post-curing. Rohacell® IG-71 is a polymethacrylimide, rigid, bromine and halogen 100% closed cell isotropic foam, has high strength-to-weight ratio, outstanding creep compression resistance, good fire properties, is non-toxic, and possesses low smoke density [8]. Details on the properties of the foam cores as provided by the manufactures are listed in Table 1.

DA4518U/PX33/150 graphite/epoxy prepregs supplied by APCM LLC were used to construct four-facesheet thickness groups each comprised of four, eight, sixteen, and thirty-two cross-ply layers. The four, eight, sixteen and thirty-two layers produced 0.110-cm, 0.224-cm, 0.447-cm and 0.894-cm thick facesheets, respectively. The facesheet thicknesses are henceforth referred to as *thin*, *medium*, *medium-thick* and *thick* facesheets, respectively. A SC-15 epoxy system (Applied Poleramics Inc.) and micro balloon (glass powder) mixture was used to bond the facesheets and the foam cores together. The three different foam cores were each used to construct sandwich panels with varying facesheet thickness and foam core density. The prepregs were co-cured with the core in a compression-molding machine. Specimens of 10.16-cm x 10.16-cm dimensions were cut from the cured panels.

Damage assessment was visually and microscopically performed both on the surface and within the specimens. Cross-sectioning the specimens longitudinally through the mid-section of the impact point carried out internal evaluation of damage. Buehler Isomet Low Speed Saw equipped with 12.7-cm diameter diamond wafering blade of less than 1-mm thickness

was used to cut the samples. The thinness of the blade (< 1-mm) ensured precise sectioning and less damage to the specimens.

Table 1. Properties of the foam cores

Property	Airex R63.5	Rohacell IG-71	Airlite B12.5
Density (kg/m^3)	60	75	200
Compression Strength (N/mm^2)	0.38	1.5	5.0
Tensile Strength (N/mm^2)	0.9	2.8	6.3
Elastic Modulus (N/mm^2)	30	92	178
Shear Strength (N/mm^2)	0.5	1.3	3.5
Shear Modulus (N/mm^2)	11	29	81
Core Thickness (cm)	1.27	1.27	1.27

Impact Testing

An Instron 8210-Drop Weight Impact Testing Machine equipped with Dynatup 930I-data acquisition system and a pneumatic clamping fixture was used to conduct the tests. To insure repeatability, three samples from each facesheet thickness and core density group were tested. The impact energy was varied according to the following sequence: 11 J, 28 J, and 40 J.

RESULTS AND DISCUSSION

Interpretation of the low velocity impact results was accomplished by using published methods [9-18].

I. Effect of Facesheet Thickness

Airlite B12.5 foam core: The effect of facesheet thickness on the impact response of Airlite B12.5-foam core specimens is presented in Figure 1 for three different impact energies: 11 J, 28 J and 40 J. For all the three impact energies considered, it can be seen from the figures that the P_m, E_m, E_t and E_t/E_{imp} impact parameters displayed increasing trends, whereas the δ_m and t_m decreased with increase in facesheet thickness. Increase in the values of P_m, E_m, E_t and E_t/E_{imp} with facesheet thickness indicates improvement in energy absorption capability of the specimens. The δ_m and t_m continuously decreased with increase in facesheet thickness because of accompanied increase in facesheet stiffness. The E_t/E_{imp} ratios of all the three-impact energies (11 J, 28 J and 40 J) approached unity with increase in facesheet thickness. Thus indicating that the specimens absorb all of the imparted energy.

The failure characteristics and damage evolution in Airlite B12.5-core specimens is presented in Figure 2. The number of fabric layers per facesheet is placed directly above the corresponding macrographs. The failure characteristics included facesheet damage in the form of fiber breakage and indentation of the upper skin, core failure (localized crushing of the core in the form a V-notch groove and distributed compression of the core), and delamination. The extent of fiber breakage decreased with increase in facesheet thickness; and failure was primarily by a combination of localized facesheet indentation and distributed compression of the core at thicker facesheets. Core compression remained visible even though the extent of fiber breakage lessened with increase in facesheet thickness.

Airex R63.5 foam core: The failure characteristics and damage evolution at different impact energies are presented in Figure 3 as a function of facesheet thickness. Core fracture just below the core-facesheet interface (i.e. below the bond line) was observed on thicker facesheet specimens; see Figure 3(a): 32-layers. Localized crushing of the foam in the form of a V-notched groove was mainly observed at on *thin* and *medium* facesheet specimens. Extensive fiber breakage, facesheet perforation, delamination and core crushing can be

observed from the macrographs. The extent of core perforation and fiber breakage can be seen to decrease with increase in facesheet thickness. Specimens with facesheets larger than the threshold thickness (i.e. $t \geq t_{threshold}$) incurred minimal damage, thus signaling that maximum deformation occur at the threshold facesheet thickness.

Rohacell IG-71 foam core: The failure characteristics and impact response of the less dense Rohacell IG-71 and Airex R63.5-foams were remarkably similar. The failure characteristics and damage evolution as a function of facesheet thickness and impact energy are presented in Figure 4 for Rohacell IG-71-foam core specimens. Similarities in failure characteristics between Rohacell IG-71 and Airex R63.5-foam specimens are apparent from Figures 3 and 4. The impact response of the less Airex R63.5 and Rohacell IG-71 foams is presented next using representative results from Rohacell IG-71-foam core specimens.

Within the impact energy range and facesheet thicknesses considered in this study, the impact response of the δ_m and t_m parameters for the less dense Airex R63.5 and Rohacell IG-71-foams was strongly sensitive to facesheet thickness as well as impact energy level; i.e. the general trends of the impact parameters were different for different combinations of facesheet thickness and impact energy.

At lower impact energy (11 J): Generally, the impact parameters increased with facesheet thickness in a parabolic manner up to a point and thereafter decreased or leveled-off, see Figure 5. It can be seen from the figures that the P_m, E_m, E_t, t_m and E_t/E_{imp} impact parameters increased up to a maximum, and thereafter decreased or leveled-off. The δ_m impact parameter decreased continuously with facesheet thickness. The maximums (or minimums) of the impact plots correspond to the threshold facesheet thickness ($t_{threshold}$), which is indicated on the plots by the faint dotted-vertical lines for the 11 J impact energy. The fact that the P_m, E_m, E_t, and E_t/E_{imp} ratios are maximum at the threshold thickness indicates that energy absorption is maximized at the threshold facesheet thickness. Whereas a decrease in the values of the δ_m and t_m after the threshold thickness indicates that flexibility is lost because of increased facesheet stiffness. Therefore, both flexibility and improved impact damage resistant is attained when the facesheet thickness is increased below the threshold thickness ($t \leq t_{threshold}$). In this case, flexibility and impact damage resistance is maximized at the threshold facesheet thickness. The threshold facesheet thicknesses were comparable among the E_t, t_m and E_t/E_{imp} impact parameters and were approximately 4.7-mm (17 fabric layers). The $t_{threshold}$ for the P_m and E_m impact parameter was about 6.7-mm (24 fabric layers).

For Airex R63.5-foam specimens, the threshold facesheet thicknesses were comparable among the E_t, δ_m, t_m and E_t/E_{imp} impact parameters and were approximately 2.8-mm (10 fabric layers). The $t_{threshold}$ for the E_m impact parameter was about 4.7-mm (17 fabric layers).

At higher impact energies (28 J and 40 J): The impact response of the P_m, E_m, E_t and E_t/E_{imp} impact parameters followed similar increasing trends for all the three impact energies (11 J, 28 J and 40 J). Depending on the impact energy level, the δ_m and t_m impact parameters either increased or decreased with facesheet thickness; see Figure 5. The δ_m and t_m impact parameters decreased in a parabolic manner at lower impact energy (11 J) and increased at higher impact ones (28 J and 40 J). The results indicate that core compression is enormous at high impact energies. The total energy-to-impact energy (E_t/E_{imp}) ratios of all the three-impact energies (11 J, 28 J and 40 J) approached unity with increase in facesheet thickness. Thus further indicating that the energy absorption capacities of the specimens max out with continuous increase in facesheet thickness. The effect of increased in impact energy was to shift the P_m, E_m and E_t upward and the effect were pronounced at thicker facesheets. However, the δ_m and t_m impact parameters shifted downward and the influence of impact energy level was pronounced at thinner facesheets.

For all three-foam cores: Depending on the impact energy level, the impact parameters varied either linearly, parabolically up to a point, sinusoidally or exponentially with facesheet thickness. The P_m, E_m, E_t/E_{imp} and E_t impact parameters increased with facesheet thickness for all the three foam-core specimens. Whereas, the δ_m and t_m decreased with facesheet thickness for the denser Airlite B12.5-foam core specimens, and either increased or decreased for the less dense Rohacell IG-71 and Airex R63.5 foams depending on the impact energy level.

For all three foam-core specimens, the E_t/E_{imp} ratios increased asymptotically with facesheet thickness and approached unity; see Figures 1 and 5. Thus indicating that, with continued increase in facesheet thickness far beyond critical thickness, the total energy per impact energy ratio would not be influenced by facesheet thickness and that energy absorption max out; core crushing initiates at all facesheet thicknesses though. An increase in the values of E_t/E_{imp} indicates an increase in the energy absorption capacity of the material. The value of unity indicates that the specimen absorbed all of the imparted energy. The influence of impact energy on the E_t/E_{imp} impact parameter was pronounced at thinner facesheets, especially for the less dense Rohacell IG-71 and Airex R63.5-core specimens. All three foam-core specimens displayed lower values of E_t/E_{imp} ratios at thinner facesheets, thus signaling less impact damage resistant. The Airlite B12.5 foam-core, which is the densest among the three foams, exhibited superior energy absorption capacity.

Damage in the form core fracture near the core-facesheet interface was observed on thicker facesheets (0.894-cm thick or 32 layers) specimens of the less dense Rohacell IG-71 and Airex R63.5 foams. Core fracture below the bond-line was due to compression core crushing, which was magnified because of the inertial effects of thicker facesheets. A massive load drop (first major load drop) was observed on the load-time traces of the thicker facesheet specimens, and was accompanied on the macrographs by either core fracture below the bond-line or delamination. Core fracture just below the core-facesheet interface was not observed on Airlite B12.5 thicker facesheet specimens; only pure delamination was observed.

Damage to the facesheet was significantly reduced with increase in facesheet thickness; failure was primarily by a combination of distributed core compression and interface delamination at thicker facesheets. Consequently, localized foam core crushing also decreased. Thus, indicating that failure was dominated by distributed compression of the core at thicker facesheets as opposed to localized compression in the form of V-notched groove. Core compression remained visible even though the extent of fiber breakage lessened with increase in facesheet thickness. Localized crushing of the core was mainly observed at thinner facesheets. At very thick facesheets (8.9-mm), small indentation on the facesheet, distributed core compression and core fracture below the bond-line were the primary operative failure mechanisms. Core fracture just below the facesheet/core interface at thicker facesheets was due to core compression, which was magnified because of the inertial effects of thicker facesheet.

For the denser Airlite B12.5-foam core specimens, the general trends of the P_m, E_m, E_t, E_t/E_{imp}, δ_m and t_m impact parameters as a function of facesheet thickness were the same for all the three impact energy levels considered, i.e. 11 J, 28 J and 40 J. The trends were strongly dependent on the impact energy level for the less dense Rohacell IG-71 and Airex R63.5-foam core specimens.

II. Effect of Foam Core Density

Compared to Airex R63.5 and Rohacell IG-71-foam core specimens, the Airlite B12.5-foam core specimens sustained less damage to the core and facesheet for a given impact energy. Perforation and crushing of the core, and fiber breakage was minimal in Airlite B12.5-foam core specimens because of the high compressive strength, tensile strength and elastic modulus

of the Airlite B12.5 foam, see Table 1. The denser Airlite B12.5 foam stretched and compressed less prior to core-compression failure because of its high compressive strength. See Figure 2 for the failure characteristics and damage evolution in Airlite B12.5-foam core specimens. Denser foam (Airlite B12.5) improved the impact damage resistance of the sandwich specimens; thus resulting in specimens that were able to deflect more prior to compression failure of the core because of reduced damage.

For the less dense Airex R63.5 and Rohacell IG-71-foam core specimens, a greater part of the energy was expended in initiation and progression of damage, see Figures 3 & 4 for failure characteristics and damage evolution, respectively. The less dense Airex R63.5 and Rohacell IG-71 foams stretched and compressed significantly prior to core-compression failure because of their low compressive strength, tensile strength and elastic modulus as compared to Airlite B12.5 foam, see Table 1. The compression strength of Airlite B12.5 foam (5 N/mm^2) is about thirteen times that of Airex R63.5 foam (0.38 N/mm^2) and three times that of Rohacell IG-71 foam (1.5 N/mm^2). Therefore, Airlite B12.5 foam core stretched less prior to compression failure as compared to Airex R63.5 and Rohacell IG-71 foam cores because of its higher compression strength. Also, it should be noted that the composition of Rohacell IG-71 foam is different from that of Airlite B12.5 and Airex R63.5 foams, which are both PVC foams, but has density closer to that of Airex R63.5 foam.

The influence of foam core on the impact response of different impact parameters is presented in the following sections as a function of facesheet thickness and impact energy.

(a) Facesheet thickness

The P_m and E_m impact parameters: The influence of foam core density on the P_m and E_m impact parameter is presented in Figure 6 for the 11 J, 28 J and 40 J impact energies. For all three-impact energies, the values of the P_m impact parameter for the denser Airlite B12.5-foam core specimens were higher than those of Rohacell IG-71 and Airex R63.5-foam core specimens; thus indicating superior impact resistance, Figures 6(a)–(c).

The E_m impact parameter exhibited a transition point, below which the values of the E_m impact parameter were higher for the denser Airlite B12.5-foam core specimens as compared to the less dense Rohacell IG-71 and Airex R63.5-foam ones, and vice versa. The transition point corresponds to the critical or minimum facesheet thickness ($t_{critical}$) required for the less dense-foam core (Rohacell IG-71 and Airex R63.5) specimens to have comparable or better impact properties than those of the denser-foam core (Airlite B12.5) specimens. The critical facesheet thicknesses at different impact energies are indicated on the impact plots by the dotted-vertical lines, see Figure 6(d)-(f). A transition from denser to less dense-foam core dominated impact response (or vice versa) occurs at the critical facesheet thickness. The critical facesheet thickness for the E_m impact parameter is indicated on the figures by the dotted-vertical lines, and is 6.7-mm (24 layers) for the 11 J, and 7.8-mm (28 layers) for the 28 J & 40 J impact energies. The lower values of the E_m impact parameter for the less dense Rohacell IG-71 and Airex R63.5-foam specimens at *thin* facesheets, i.e. less than the critical thickness, was due to extensive deformation sustained by these specimens. Again, the closeness between the impact response of Rohacell IG-71 and Airex R63.5-foam core specimens can be noticed from the Figures 6(a)-(f).

The E_t and E_t/E_{imp} impact parameters: Below the critical facesheet thickness, the E_t and E_t/E_{imp} impact parameters of the denser Airlite B12.5-foam specimens were higher than those of the less dense Rohacell IG-71 and Airex R63.5-foam core specimens, see Figure 7(a)-(f). The influence of the type of foam core was not apparent at thicker facesheets; the values of the E_t and E_{imp} impact parameters were comparable among all the three foam-core specimens at 16-layer and 32-layer facesheets. It can be seen from the figures that the E_t and E_t/E_{imp} impact parameters of the three foam core specimens converged to a common value with increase in facesheet thickness. The E_t/E_{imp} impact parameters of the different foam core

specimens also approached unity at thicker facesheets; see Figures 7(d)-(f). The lower values of the E_t/E_{imp} ratios at thinner facesheets, less than unity, indicate that less energy is absorbed by the specimens or is absorbed primarily by the foam core.

Similarly, the critical facesheet thickness ($t_{critical}$) for the E_t and E_t/E_{imp} impact parameters is indicated on the plots by the dotted-vertical lines; which is 2.2-mm (8 layers) for the 11 J, and 7.3-mm (26 layers) for the 28 J & 40 J impact energies, see Figures 7(a)-(f). Above the critical thickness, the disparity in the E_t and E_t/E_{imp} impact response among the different foam-core specimens or dominance of E_t and E_t/E_{imp} impact parameters by a particular foam core is minimal. The impact damage resistance of the less dense (Rohacell IG-71 and Airex R63.5) foam core specimens improved with increase in facesheet thickness. Consequently, the less dense foam specimens with thicker facesheets sustained lesser damage; as a result, the values of their E_t and E_t/E_{imp} impact parameters became comparable to those of the denser foam core specimens. It should be noted that, for a given impact energy, the critical facesheet thickness for the E_t and E_t/E_{imp} impact parameters were comparable.

The t_m and δ_m impact parameters: The δ_m and t_m impact parameters exhibited a decreasing trend with facesheet thickness for the denser Airlite B12.5-foam specimens and an increasing one for the less dense Rohacell IG-71 and Airex R63.5-foam specimens, see Figures 8(a)-(f). The impact response of the δ_m and t_m impact parameters as a function of facesheet thickness was different at lower (11 J) and higher impact energies (28 J and 40 J). At lower impact energy, the δ_m and t_m varied in a sinusoidal manner for the denser Airlite B12.5-foam specimens but increased parabolically up to a point for the less dense Rohacell IG-71 and Airex R63.5-foam specimens. At higher impact energies, the δ_m and t_m impact parameters displayed a parabolic decrease for the denser Airlite B12.5-foam specimens, and an exponential increase for the less dense Rohacell IG-71 and Airex R63.5-foam specimens.

The critical facesheet thickness for the δ_m and t_m impact parameters increased with facesheet thickness; and was 1.4-mm (5 layers), 3.6-mm (13 layers) & 6.7-mm (24 layers) for the 11 J, 28 J & 40 J impact energies, respectively. The critical facesheet thickness is indicated on the plots by the dotted-vertical lines. Note that, for a given impact energy, the critical facesheet thicknesses for the δ_m and t_m impact parameters were comparable. Beyond the critical facesheet thickness, the values of the δ_m and t_m impact parameters were higher for the less dense Rohacell IG-71 and Airex R63.5-foam specimens as compared to the denser Airlite B12.5-foam specimens. Thus indicating that the less dense foam cores are favorable for thicker facesheet specimens, $t \geq t_{critical}$, and vice versa.

The maximums (or minimums) of the P_m, E_m, E_t, δ_m, t_m and the inflection points of the E_t/E_{imp} impact parameters correspond to the threshold facesheet thickness, $t_{threshold}$. The threshold facesheet thickness generally increased with impact energy. The minimums and maximums of the δ_m and t_m impact parameter are related to the change in the primary mode of failure. The primary mode of failure changed from breakage of the facesheet fibers and localized crushing of the core in the form a V-notched groove to mainly failure by delamination and distributed compression of the core. Delamination was due to inertial effects resulting from thicker facesheets.

(b) Impact energy

The P_m and E_m impact parameters: Compared to the less dense Airex R63.5 and Rohacell IG-71-foam specimens, the values of the P_m and E_m impact parameters were higher for the denser Airlite B12.5-foam core specimens; i.e. the impact parameters improved with increase in density, see Figure 9(a)–(h). The effect of the type of foam core on the E_m impact parameter was pronounced at higher impact energies, Figures 9(e)-(h).

The critical impact energy ($E_{critical}$) is indicated on the plots by the dotted-vertical lines, see Figures 9(g) & (h). The critical impact energy is a transition point and corresponds to the energy at which the impact response changes from being dominated by a denser-foam to being less dense-foam dominated (or vice versa); see Figure 9(d). The $E_{critical}$ corresponds to the intersections of the impact plots of Airlite B12.5, Airex R63.5 and Rohacell IG-71-foam specimens. Below the $E_{critical}$, the values of the E_m impact parameter are comparable among the three foam-core specimens, i.e. Airlite B12.5-foam, Rohacell IG-71-foam and Airex R63.5-foam specimens. Thus indicating that the disparity in the impact response of the E_m impact parameter among the different foam-core specimens or dominance of E_m by a particular foam core is minimal below the critical energy. The critical impact energy of the P_m impact parameter was only observed at very large facesheets; i.e. the type of foam core influences the impact response of the P_m impact parameter even at very large facesheet thicknesses (8.9-mm).

The maximums (or minimums) of the P_m, E_m, E_t, δ_m and t_m and the inflection points of the E_t/E_{imp} impact parameters correspond to the threshold impact energy, $(E_{imp})_{threshold}$. Examples of the threshold impact energies are illustrated in Figures 9(c) & (e) for the P_m and E_m impact parameters. The results indicate that the energy absorption is either maximized or minimized at the threshold impact energies.

A comparison between sandwich specimens made from the same family of foam cores, i.e. Airlite B12.5 and Airex R63.5 foam, is presented in Figure 9(a) & (e) for *thin* facesheets specimens. It can be seen from the figures that, throughout the impact energy range, the P_m and E_m impact parameters are higher for the denser Airlite B12.5-foam core specimens; i.e. the impact parameters improved with increase in density. The results indicate that within the same family of foam cores, the denser foam core yield improved impact properties.

The E_t and E_t/E_{imp} impact parameters: The critical impact energy of the E_t and E_t/E_{imp} impact parameters increased with increase in facesheet thickness. Higher critical energy means that there are wider ranges of impact energies within which the E_t and E_t/E_{imp} impact parameters of the different foam specimens are comparable. Below the critical impact energy level, the E_t and E_t/E_{imp} ratios were the same for all three foam-core specimens; the impact response of these parameters was less sensitive to the type of foam core and was more controlled by the facesheet, see Figures 10(a)-(h).

The E_t and E_t/E_{imp} impact parameters were not sensitive to the type of foam core at very thick facesheets; see Figure 10(d) and (h). At larger facesheet thicknesses, the impact response was mainly controlled by the facesheet as failure was primarily by indentation of the facesheet and distributed compression of the core. The core primarily experiences distributed compressive loading at very thick facesheets as opposed to concentrated loading that resulted in perforation at thinner facesheets. Damage to the facesheet in the form of fiber breakage was not observed at thicker facesheets; only a small indentation on the surface of the facesheets was observed.

The impact parameters of the three foam-core specimens were comparable at thicker facesheets, thus indicating that the type of foam core becomes critical in energy absorption for thinner facesheet sandwich composites, see Figure 10(d) and (h). Even though the energy absorbed is a combined influence of the individual constituents, the impact response becomes more facesheet controlled at larger facesheet thicknesses. The specimens were not able to deflect easily because of increase in facesheet thickness, hence facesheet stiffness; therefore damage was more in the facesheet and less by core deflection. Core compression was magnified though. The influence of foam core was pronounced at thinner facesheets for all the three foam cores.

The δ_m and t_m impact parameters: The δ_m and t_m impact parameters varied parabolically or hyperbolically with impact energy. Below the critical energy, the values of the δ_m and t_m were higher for the less dense foam (Airex R63.5 and Rohacell IG-71 foams) specimens as compared to the denser one (Airlite B12.5 foam), see Figures 11(a)-(h). Thus indicating that the less dense-foam cores controlled the δ_m and t_m impact parameters at impact energies that were below the critical energy. At thicker facesheets, perforation of the facesheet and localized crushing of the core was reduced because the compressive loads were more distributed to the core by the thicker (*medium-thick*) facesheets. Flexure of the specimens was more by core deflection and less by facesheet deflection at thicker facesheets; as a result, the less dense-foams dominated the impact response at impact energies that were below the critical energy. The impact behavior of the δ_m and t_m parameters was completely controlled by the less dense-foam core at very thick facesheets (8.94-mm thick or 32 plies), Figures 11(d) and (e). The critical impact energies of the δ_m and t_m impact parameters increased with facesheet thickness.

In summary, the P_m, E_t/E_{imp} ratios, and E_t impact parameters exhibited increasing trends with increase in facesheet thickness (number of fabric layers) for all the three foam core specimens (i.e. Airlite B12.5, Rohacell IG-71 and Airex R63.5 foams). Whereas, the E_m, δ_m, and t_m either increased or decreased parabolically or varied sinusoidally depending on impact energy and type of foam core. The type of foam core mainly controlled the impact behavior of the E_m, δ_m and t_m impact parameters and had less influence on the E_t and E_t/E_{imp} impact parameters at thicker facesheets. Below the critical energy, the E_m, δ_m and t_m impact parameters were higher for the less dense foam core specimens. The results from all three-impact energies (11 J, 28 J & 40 J) indicate that it is advantageous to utilize a denser foam cores at thinner facesheets, i.e. less than critical thickness, and vice versa. The critical impact energy increased with facesheet thickness.

The P_m, E_m and E_t impact parameters exhibited increasing trends and, the E_t/E_{imp} ratios decreased with impact energy for all three foam specimens and facesheet thicknesses (0.110-cm to 0.894-cm) considered in this study. The δ_m and t_m either increased or decreased with impact energy depending on the facesheet thickness and type of foam core.

Generally, the critical ($t_{critical}$) and threshold ($t_{threshold}$) facesheet thickness displayed increasing trends with increase in impact energy. Deflection and energy absorption is either maximized or minimized at the threshold impact energy. The critical impact energy ($E_{critical}$) generally increased with facesheet thickness, whereas the threshold impact energy ($E_{threshold}$) did not exhibit clearer trends with facesheet thickness. Repeatability of the impact response and results data was excellent among all the three-foam core specimens. Inconsiderable amount of scatter in data was perceived.

III. Effect of Impact Energy

For Airlite B12.5-foam specimens, the P_m, E_m, E_t, δ_m and t_m generally increased with impact energy, whereas E_t/E_{imp} ratios exhibited a decreasing trend. The general trends of the impact parameters as a function of impact energy were similar for the different facesheet thicknesses considered. At lower impact energies (11 J), the E_t and E_t/E_{imp} impact parameters were insensitive to increase in facesheet thickness; the influence of facesheet thickness was apparent mainly at higher impact energies. Increasing the facesheet thickness shifted the P_m, E_m, E_t and E_t/E_{imp} impact parameters upward, but lowered the δ_m and t_m. Scatter in data was mainly observed in the impact plots of the δ_m and t_m impact parameters. The extent of damage increased with impact energy.

CONCLUSION

The failure characteristics included facesheet damage in the form of fiber breakage; core failure (localized crushing of the foam in the form of a V-notch and distributed compression of the core), delamination and debonding near the core/facesheet interface. The threshold facesheet thickness ($t_{threshold}$), critical or minimum facesheet thickness ($t_{critical}$), threshold impact energy level $(E_{imp})_{threshold}$, and critical energy ($E_{critical}$) were identified from the impact plots. The impact parameters varied linearly, parabolically or sinusoidally with impact energy depending on the impact energy level, type of foam core and facesheet thickness. Excellent repeatability of impact response and results data was obtained, which improved further with increase in foam density and facesheet thickness.

REFERENCES

1 Akay, M. and Hanna, R., *Composites*, **21**(4), (1990) 325-331
2 Danielsson, M. and Grenestedt, J.L., *Composites Part A*, **29**(8), (1998) 981-988
3 Hall, R., *J. Comp. Mater*., **30**(17), (1996) 1939-1956
4 Nemes, J.A. and Simmonds, K.E., *J. Comp. Mater*., **26**(4), (1992) 500-519.
5 Vaidya, U.K., Rodgers, R., and Hosur, M.V., *22nd National SAMPE Technical Conference*, 2000
6 www.baltek.com
7 www.alusisse-airex.com
8 www.richmond-aircraft-prod.com
9 ASTM STP 568, *Foreign Object Impact Damage to Composites*, ASTM, Philadelphia, Pa, (1975)
10 ASTM STP 563, *Instrumented Impact Testing*, Philadelphia, Pa, (1974)
11 ASTM STP 936, *Instrumented Impact Testing of Plastics and Composite Materials*, Philadelphia, Pa, (1987)
12 Herup, E.J. and Palazotto, A.N., *Composites Science and Technology*, **57**(12), (1997) 1581-1598
13 Aggag, G. and Takahashi, K., *Polymer Engineering and Science*, **36**(17), (1997) 2260-2266
14 Motuku, M., Janowski, G.M., Vaidya, U.K., Mahfuz, H., and Jeelani, S., *Proc. ASME Noise Control and Acoustics Division*, Anaheim, California, NCA-Vol. **25**, (1998) 283-295
15 Zanichelli, C., Rink, M., Pavan, A., and Ricco, T., *Polymer Engineering and Science*, **30**(18), (1990) 1117-1124
16 Delfosse, D., Pageau, G., Bennett, R., and Poursartip, A., *Composites Technology & Research*, **15**(1), (1993) 38-45
17 Sreenivasan, P.R., *TRANS. Indian Inst. Met*., **49**(5), (1996) 677-696
18 Bezeredi, A., Voros, G., and Pukanszky, B., *Material Science*, **32**, (1997) 6601-6608

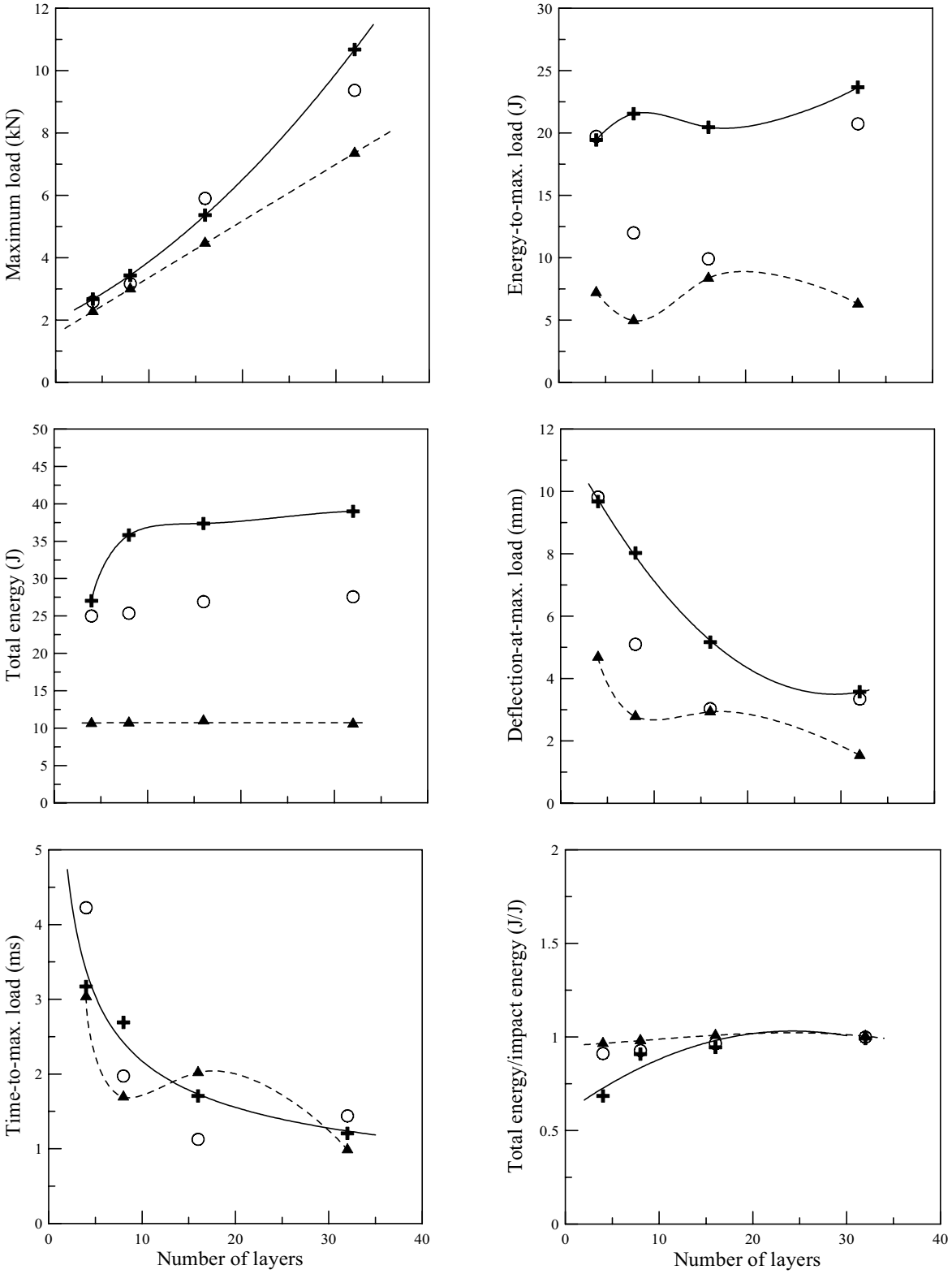

Fig. 1. Effect of facesheet thickness at different impact energy levels of 🚗: 11 J, 🚚: 28 J and ✂: 40 J for Airlite B12.5- core specimens.

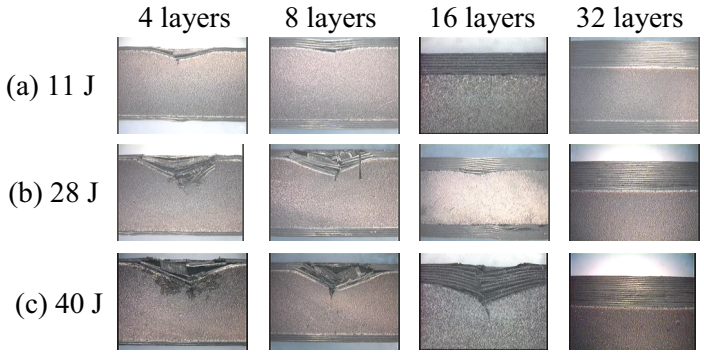

Fig. 2. The effect of impact energy and damage evolution in Airlite B12.5-foam core specimens that were impacted at 11 J, 28 J and 40 J.

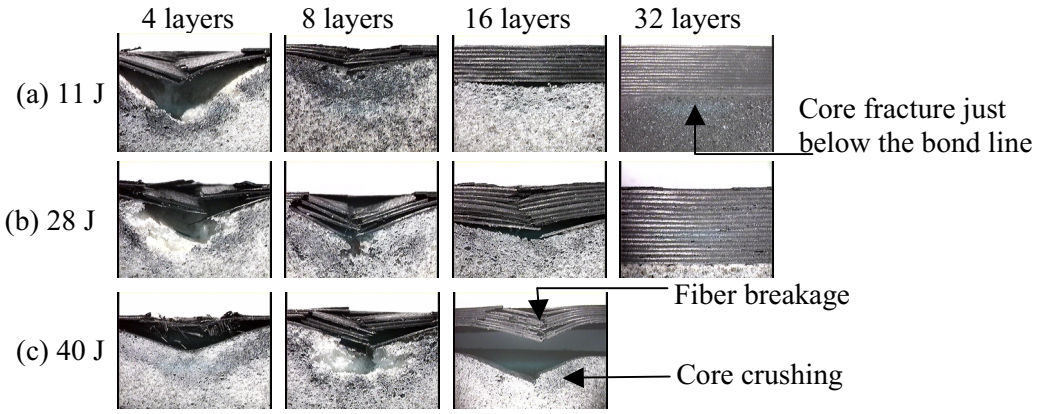

Fig. 3. Damage evolution and failure characteristics in Airex R63.5-foam core specimens that were impacted at 11 J, 28 J and 40 J.

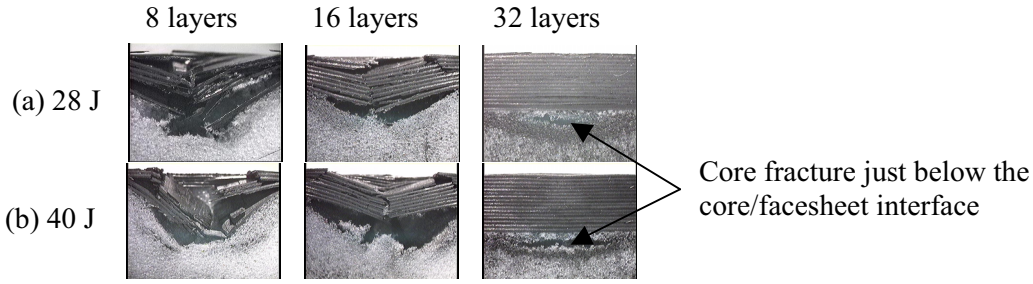

Fig. 4. Macrographs of Rohacell IG-71 foam core specimens that were impacted at 28 J and 40 J, and core fracture below the facesheet/foam core interface can be observed.

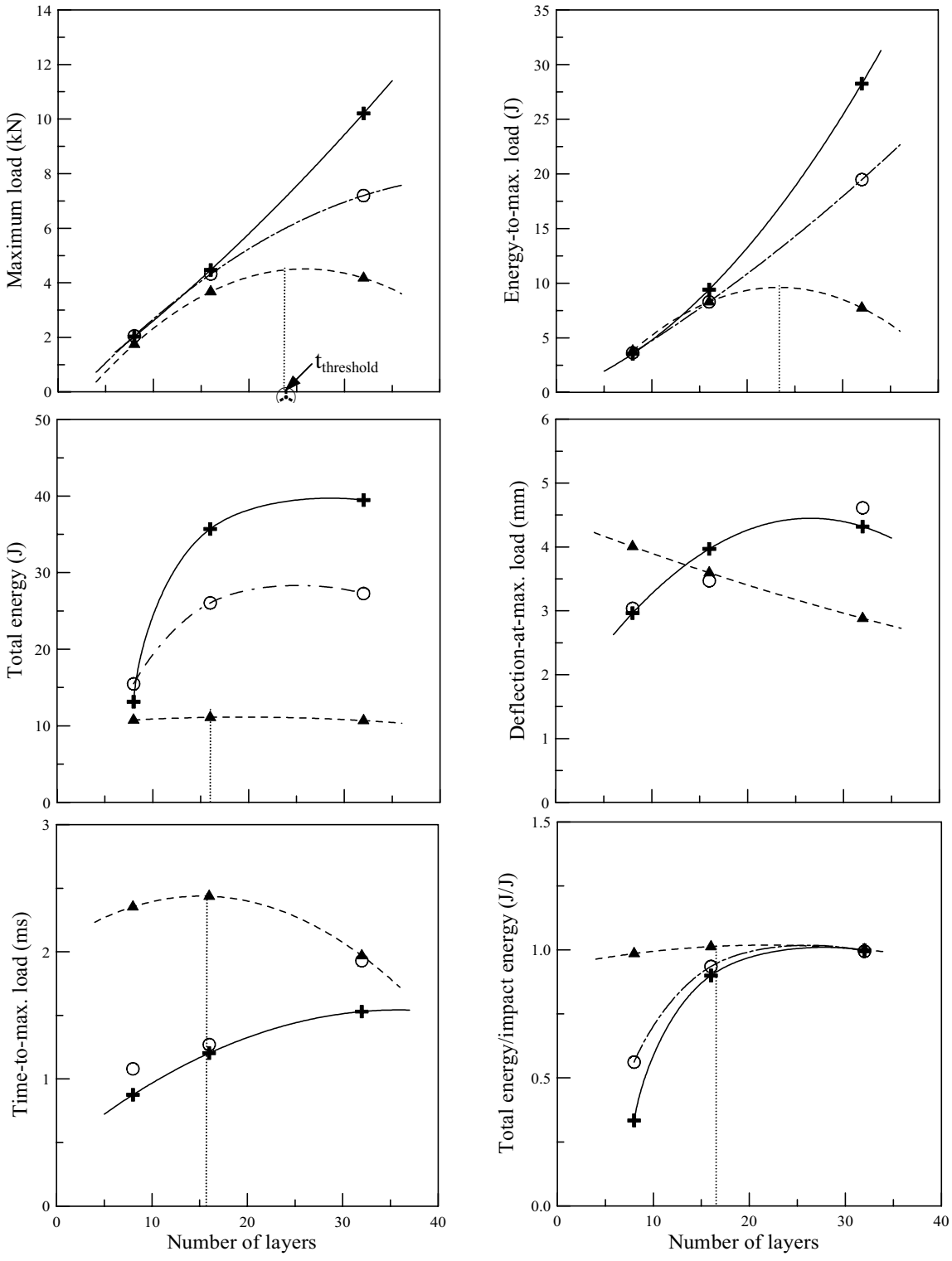

Fig. 5. Effect of facesheet thickness on impact response at different impact energy levels: 🚗: 11 J, 🖥: 28 J and ✂: 40 J for Rohacell IG-71-core specimens.

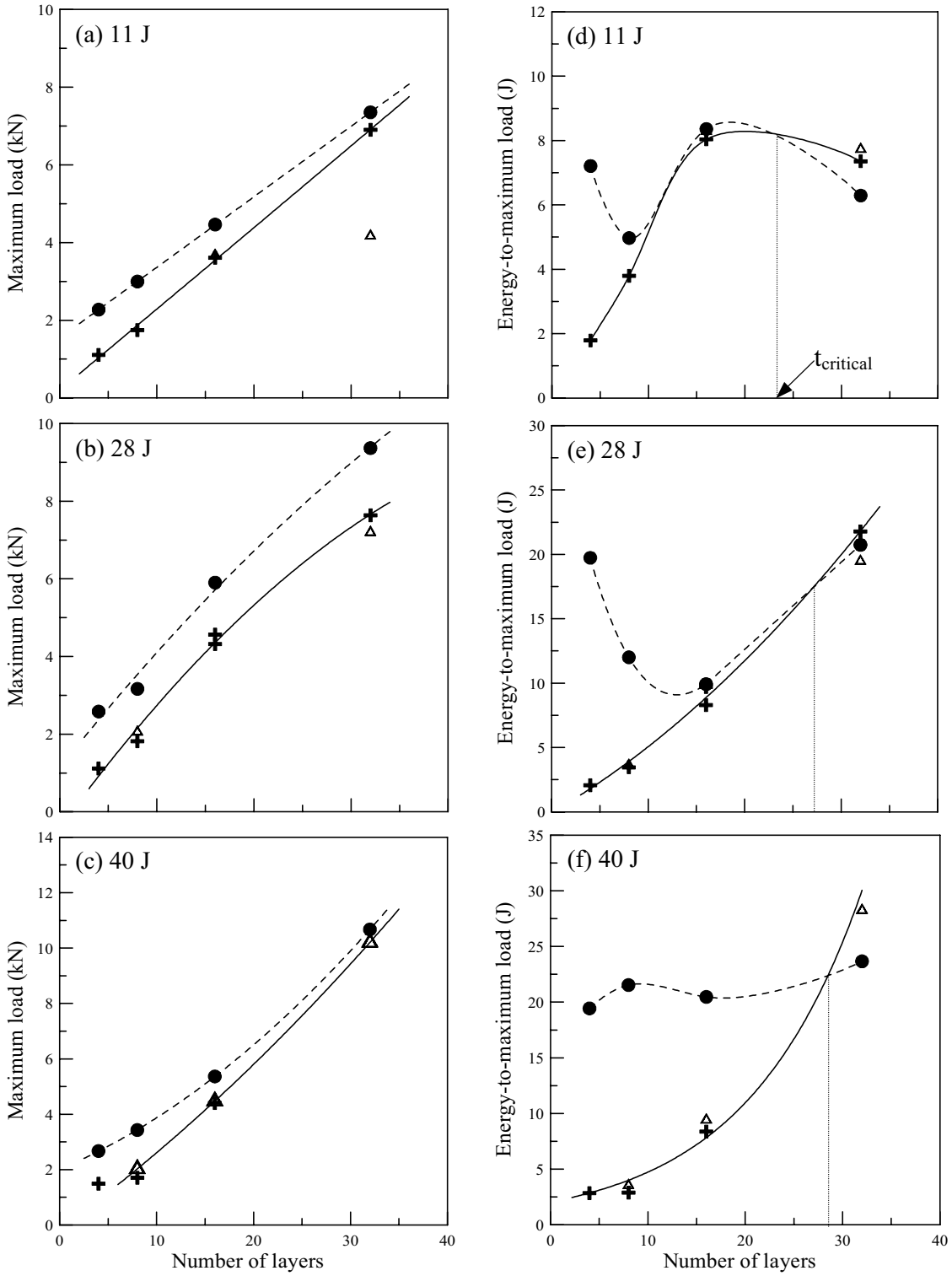

Fig. 6. Effect of foam core density on the (a)-(c) P_m and (d)-(f) E_m impact parameters at different impact energy levels of 11 J, 28 J and 40 J.
(✂: Airex Foam, 🗀: Rohacell Foam, 🚘: Airlite Foam)

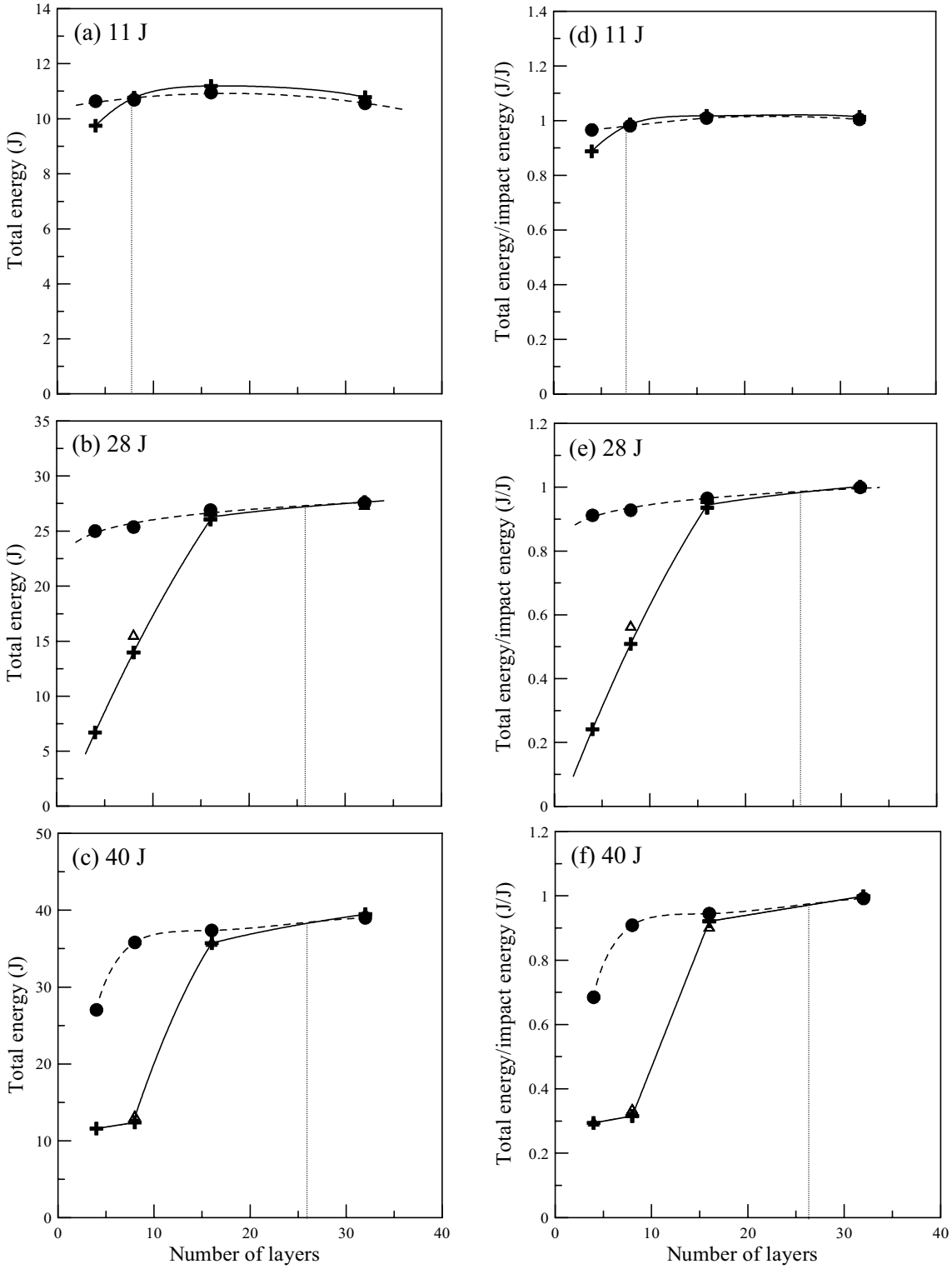

Fig. 7. Effect of foam core density on the (a)-(c) E_t and (d)-(f) E_t/E_{imp} impact parameters at different impact energy levels of 11 J, 28 J and 40 J.
(✂: Airex Foam, 🗁: Rohacell Foam, 🚘: Airlite Foam)

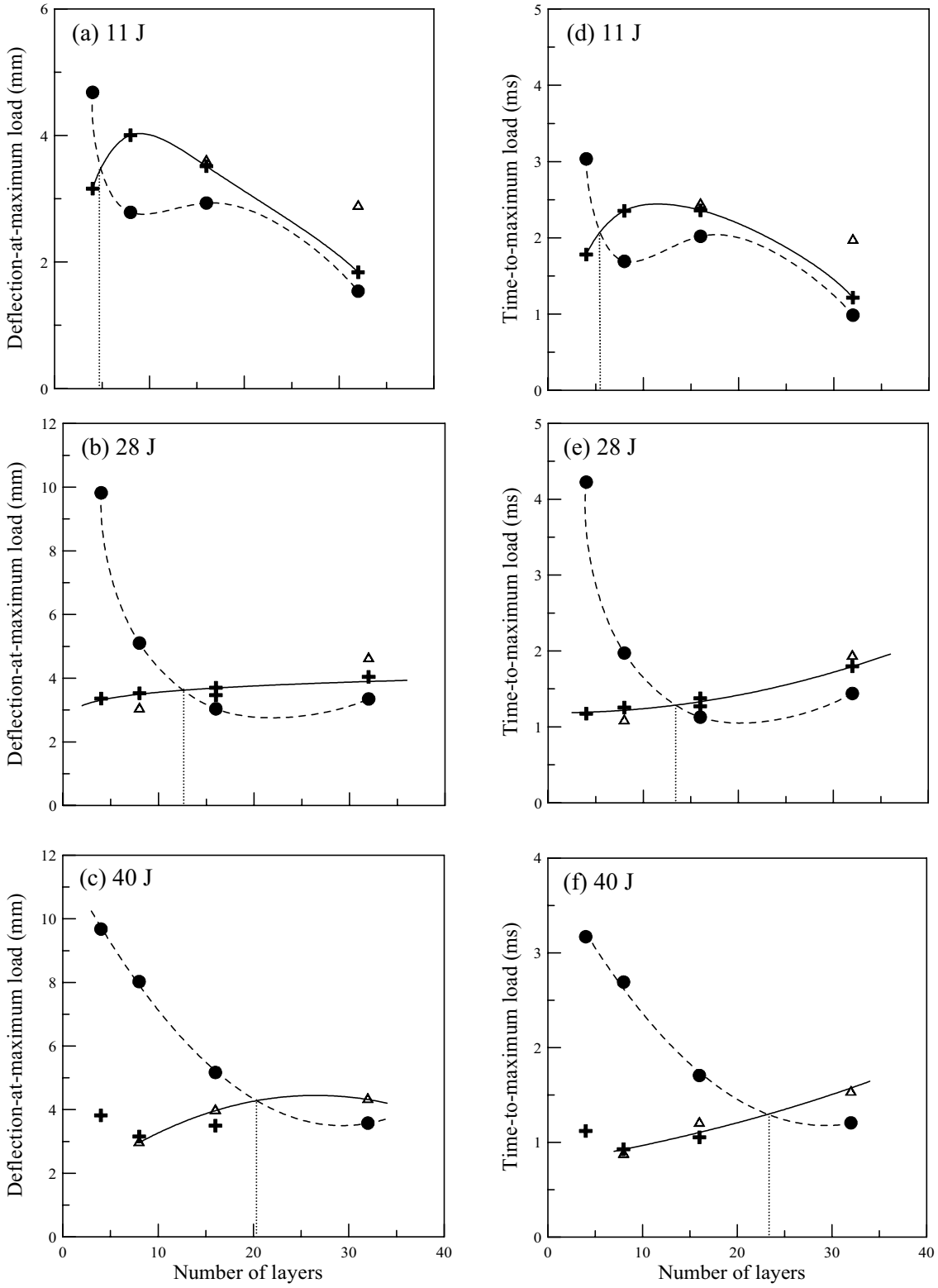

Fig. 8. Effect of foam core density on the (a)-(c) δ_m and (d)-(f) t_m impact parameters at different impact energy levels of 11 J, 28 J and 40 J.
(✂: Airex Foam, 🗁: Rohacell Foam, 🚘: Airlite Foam)

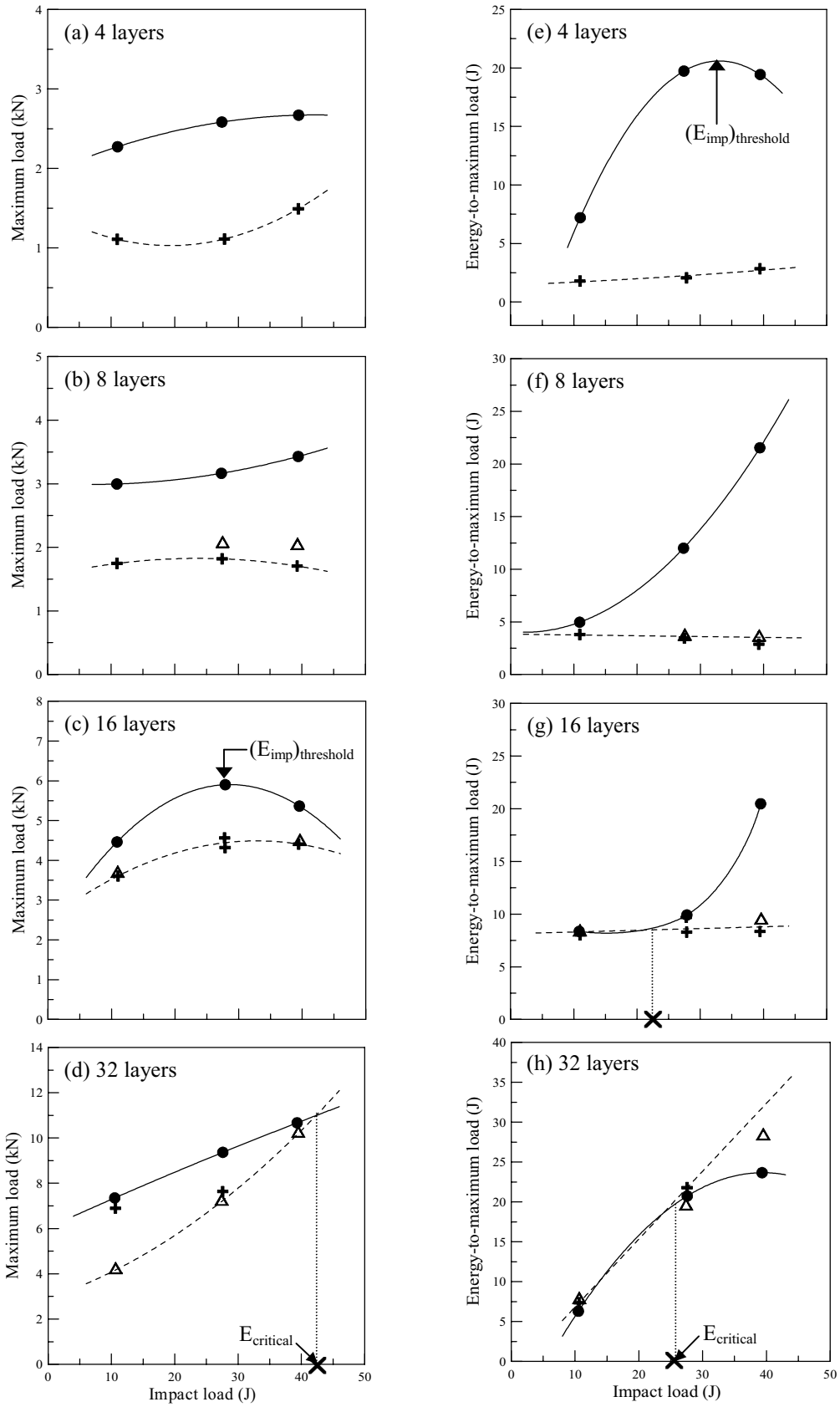

Fig. 9. Effect of foam core density and impact energy on the (a)-(d) P_m and (e)-(h) E_m impact parameters for facesheet thickness consisting of 4, 8, 16 and 32 layers of fabric.
(✂: Airex Foam, 🗀: Rohacell Foam, 🚘: Airlite Foam)

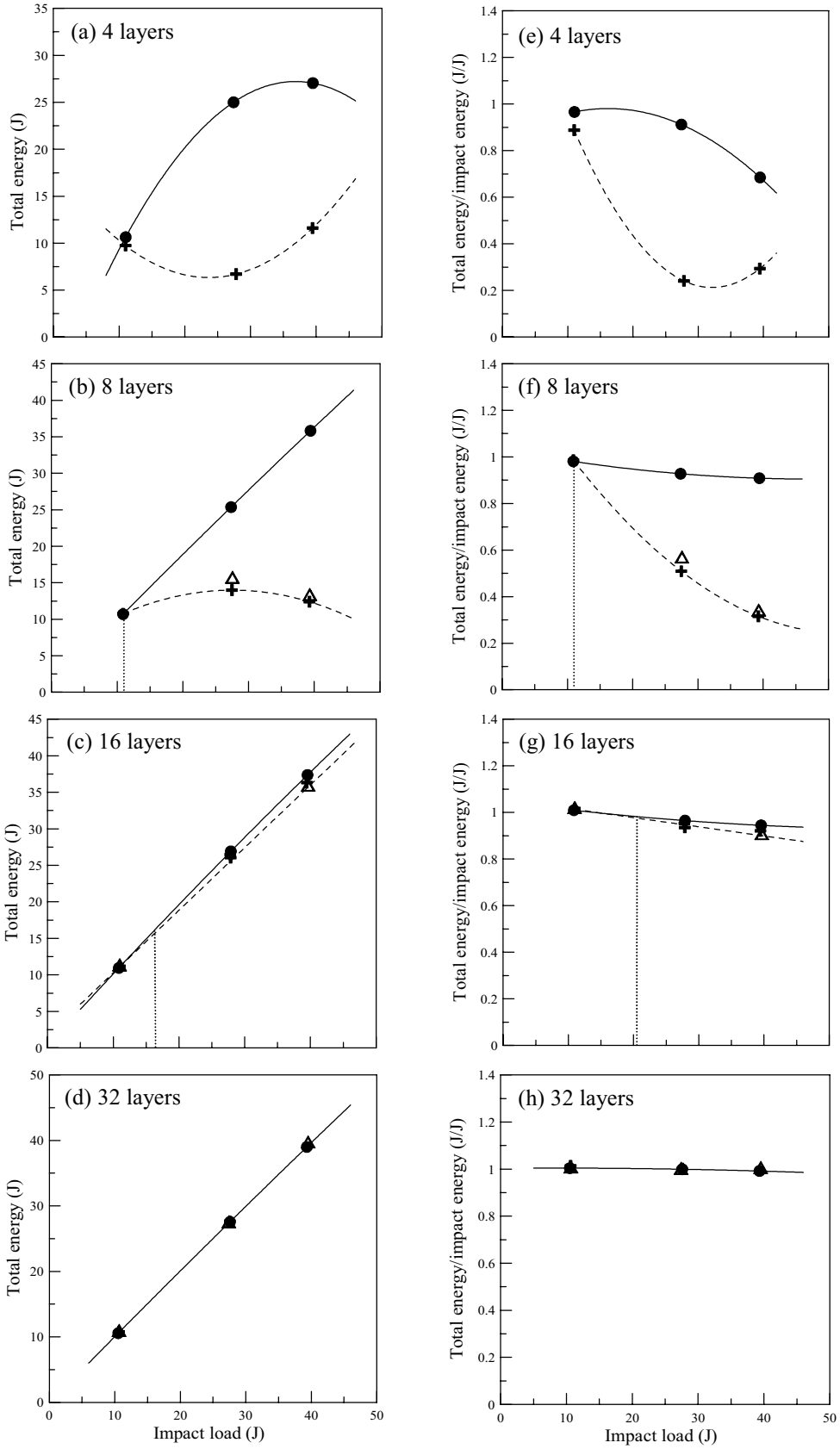

Fig. 10. Effect impact energy and of foam core on (a)-(d) E_t and (e)-(h) E_t/E_{imp} impact parameters for facesheet thickness consisting of 4, 8, 16 and 32 layers of fabric.
(✂: Airex Foam, 🗁: Rohacell Foam, 🚘: Airlite Foam)

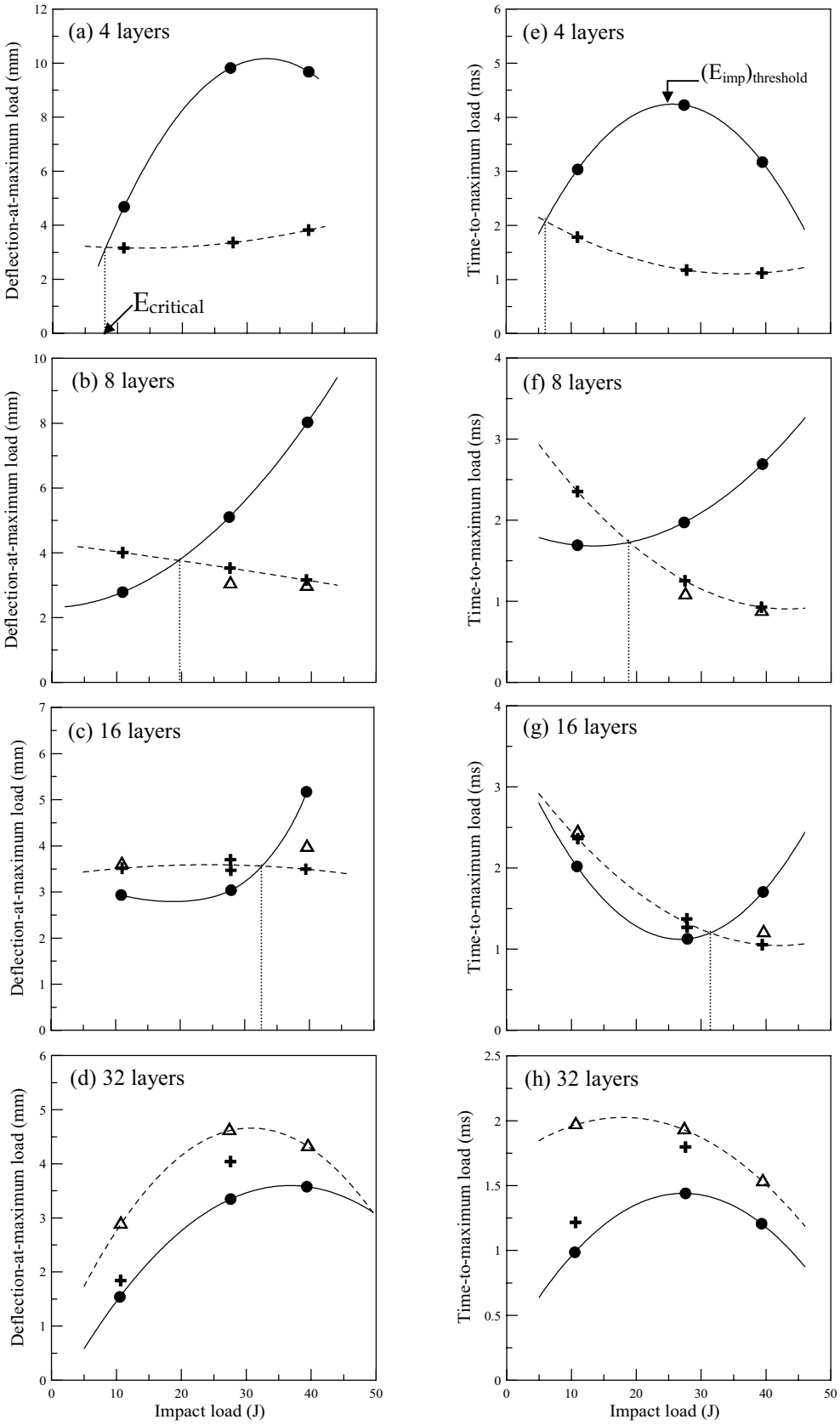

Fig. 11. Effect impact energy and of foam core on (a)-(d) δ_m and (e)-(h) t_m impact parameters for facesheet thickness consisting of 4-, 8-, 16- and 32 layers of fabric.
(✂: Airex Foam, 🗁: Rohacell Foam, 🖃: Airlite Foam)